

LEVEL II

AD-E300859
12
DNA 5077F

THE INCREASED ATTACHMENT DUE TO IONIZATION-INDUCED SMOG IN EMP ENVIRONMENTS

ADA 087850

Murray Scheibe
Mission Research Corporation
P.O. Drawer 719
Santa Barbara, California 93102

31 October 1979

Final Report for Period 1 April 1977-31 October 1979

CONTRACT No. DNA 001-77-C-0224

APPROVED FOR PUBLIC RELEASE;
DISTRIBUTION UNLIMITED.

THIS WORK SPONSORED BY THE DEFENSE NUCLEAR AGENCY
UNDER RDT&E RMSS CODE B322077464 S99QAXHD41109 H2590D.

Prepared for
Director
DEFENSE NUCLEAR AGENCY
Washington, D. C. 20305

S DTIC
ELECTE **D**
AUG 11 1980
D

DDC FILE COPY

80 7 30 . 044

Destroy this report when it is no longer needed. Do not return to sender.

PLEASE NOTIFY THE DEFENSE NUCLEAR AGENCY,
ATTN: TISI, WASHINGTON, D.C. 20305, IF
YOUR ADDRESS IS INCORRECT, IF YOU WISH TO
BE DELETED FROM THE DISTRIBUTION LIST, OR
IF THE ADDRESSEE IS NO LONGER EMPLOYED BY
YOUR ORGANIZATION.



UNCLASSIFIED

18 DNA
SITE

SECURITY CLASSIFICATION OF THIS PAGE (When Data Entered)

19 REPORT DOCUMENTATION PAGE		READ INSTRUCTIONS BEFORE COMPLETING FORM
1. REPORT NUMBER DNA/5077E, AD-E300859/AD-A087850	2. GOVT ACCESSION NO.	3. RECIPIENT'S CATALOG NUMBER
4. TITLE (and Subtitle) THE INCREASED ATTACHMENT DUE TO IONIZATION- INDUCED SMOG IN EMP ENVIRONMENTS	5. TYPE OF REPORT & PERIOD COVERED Final Report. Final 1 Apr 77-31 Oct 79	6. PERFORMING ORG. REPORT NUMBER MRC-R-532
7. AUTHOR(s) Murray/Scheibe	8. CONTRACT OR GRANT NUMBER(s) DNA 001-77-C-0224	10. PROGRAM ELEMENT, PROJECT, TASK AREA & WORK UNIT NUMBERS Subtask S99QAXHP411-09
9. PERFORMING ORGANIZATION NAME AND ADDRESS Mission Research Corporation P.O. Drawer 719 Santa Barbara, California 93102	11. CONTROLLING OFFICE NAME AND ADDRESS Director Defense Nuclear Agency Washington, D.C. 20305	12. REPORT DATE 31 October 1979
14. MONITORING AGENCY NAME & ADDRESS (if different from Controlling Office) D411	13. NUMBER OF PAGES 38	15. SECURITY CLASS (of this report) UNCLASSIFIED
16. DISTRIBUTION STATEMENT (of this Report) Approved for public release; distribution unlimited.	15a. DECLASSIFICATION DOWNGRADING SCHEDULE	
17. DISTRIBUTION STATEMENT (of the abstract entered in Block 20, if different from Report)		
18. SUPPLEMENTARY NOTES This work sponsored by the Defense Nuclear Agency under RDT&E RMSS Code B322077464 S99QAXHD41109 H2590D.		
19. KEY WORDS (Continue on reverse side if necessary and identify by block number) SMOG EMP Attachment		
20. ABSTRACT (Continue on reverse side if necessary and identify by block number) The increased electron attachment due to HNO ₂ production in the EMP source region is investigated. The HNO ₂ produced is found to be roughly linear with the total ionization up to an ionization value of about 2 x 10 ¹⁴ ion pairs. Above this, the HNO ₂ production is less than linear. Although the attachment to HNO ₂ was not enough to explain the lightning strokes in the Mike shot, it can affect the fields in the EMP source region. The attach- ment to other species via endothermic reactions which involve electrons which		

DD FORM 1 JAN 73 1473

EDITION OF 1 NOV 65 IS OBSOLETE

UNCLASSIFIED

SECURITY CLASSIFICATION OF THIS PAGE (When Data Entered)

406078

UNCLASSIFIED

SECURITY CLASSIFICATION OF THIS PAGE (When Data Entered)

20. ABSTRACT (Continued)

have been heated by the electric field was also investigated. It was concluded that only those reactions in which the energy change is small, such as the reactions with O_3 , HNO_2 , and H_2O_2 , hold much hope of contributing significantly to the overall attachment. The necessary experimental data for these reactions, however, is not available.

Accession For	
NTIS GRA&I	<input checked="" type="checkbox"/>
DDC TAB	<input type="checkbox"/>
Unannounced	<input type="checkbox"/>
Justification	
By _____	
Distribution/	
Availability Codes	
Dist.	Avail and/or special
A	

DTIC
ELECTE
AUG 11 1980
S D

UNCLASSIFIED

SECURITY CLASSIFICATION OF THIS PAGE (When Data Entered)

CONTENTS

	<u>Page</u>
INTRODUCTION	2
THE PRODUCTION OF HNO_3 IN THE EMP SOURCE REGION	8
INCREASED ATTACHMENT DUE TO HOT ELECTRONS	19
CONCLUSIONS	26
REFERENCES	28

INTRODUCTION

The reliability of EMP calculations depends on having accurate values for the electron and ion (both positive and negative) concentrations and for the mobilities of these charged particles. The electrical conductivity of air, which is a strong limiter of the fields produced, is proportional to the sum, over charged particle species, of the product of particle density and mobility.

The production of ionization by the gamma rays is easy to calculate as are the ratios of the simple positive ion species initially formed. The subsequent ion transformations and the electron and ion decay schemes are not so well known.

Until now, the calculations of the ion and electron densities for system purposes has been accomplished by the use of a very simple model involving only one positive ion species, n_+ , and one negative ion species, n_- , in addition to the electron density, n_e . This model can be described by the following equations:

$$\frac{dn_e}{dt} = q - \alpha_d n_e - An_e + Dn_- , \quad (1)$$

$$\frac{dn_+}{dt} = q - \alpha_d n_e - \alpha_i n_- n_+ , \quad (2)$$

$$\frac{dn_-}{dt} = An_e - Dn_- - \alpha_i n_- n_+ , \quad (3)$$

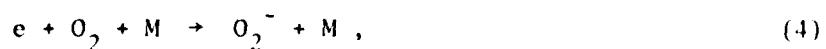
where q is the ion pair production rate, α_d is the effective electron-ion recombination (usually dissociative) coefficient, α_i is the effective ion-ion recombination coefficient, D is the effective detachment coefficient, and A is the effective electron attachment coefficient. At sea level, the detachment of electrons from negative ions is usually

negligible, except in a small volume of air very near the nuclear fireball where the radiation flux or kinetic temperature is very high, and this term is usually omitted.

The above model constitutes an enormous simplification. The actual deionization process in air can involve 50 or more ion species and almost as many neutral species, most of which are created by the deposition of energy and subsequent chemical interactions. This complexity is gathered into the effective coefficients which are usually chosen to be dependent only on temperature. In reality, they are also functions of altitude, ambient air species concentration, ionization rate and time.

For low altitudes (<30 km) and times greater than about 10^{-3} seconds, however, the electron density depends only on the ionization rate, q , and the attachment coefficient, A . Since the electron density rapidly falls much below the ion densities, the positive and negative ion densities, after a short time, are approximately equal and depend only on q and the coefficient α_i . The value of α_i is dependent on the identity of the ions involved but very little is known as to the ion identities at sea level and the individual values of α_i for these ions. The value of the effective α_i is thus usually taken to be the same for all ion combinations and there is some evidence that this is a reasonable assumption.

The attachment coefficient is, generally, the simplest of the effective rate coefficients. It can usually be associated with the three body attachment of electrons to molecular oxygen, i.e.,



where M is O_2 , N_2 or H_2O . At sea level and ambient temperature, the value of the effective attachment coefficient derived from reaction 4 is about 10^8 sec^{-1} .

There has been some reason, from observational data, to suspect that the simple air chemistry model used in EMP calculations is inadequate. We refer here to the "lightning" strokes seen in the Mike shot¹ (Figure 1) and other large yield shots. The fact that these strokes are oriented along arcs of circles centered on the burst point is convincing proof that they are driven by the EMP electric field. However, the calculated EMP fields are not large enough for these strokes to occur. One possible conclusion is that the calculated air conductivity is too high, by a factor of about four or five, in the time frame of about 0.1 to 10 milliseconds, when the lightning occurs. According to the calculations, the conductivity is primarily due to the electrons and not the ions. Given a fixed ionization rate, the only way to reduce the conductivity is to reduce the electron density; and, in the time regime in which we are operating, the only way to do this is to increase the attachment rate.

The rate coefficient of the attachment to O_2 indicated by reaction 4 is fairly well established, and its uncertainty cannot account for the factor needed to lower the electron density the amount required to explain the lightning strokes.

It is known that the chemistry following the deposition of ionizing radiation leads to the copious production of many atomic and molecular species (called smog in the trade) which are not ordinarily present in air in significant quantities. The molecular species formed include NO , NO_2 , O_3 , HO_2 , H_2O_2 , HNO_2 , and HNO_3 . NO_2 and O_3 can attach electrons with two body rate coefficients of the order of 10^{-11} cm^3/sec . This is, however, not large enough to compete with reaction 4 when even the maximum amounts of NO_2 and O_3 which can be formed are considered. Recently, however, a rate coefficient of 5×10^{-8} cm^3/sec . at 300K has been measured² for the attachment reaction



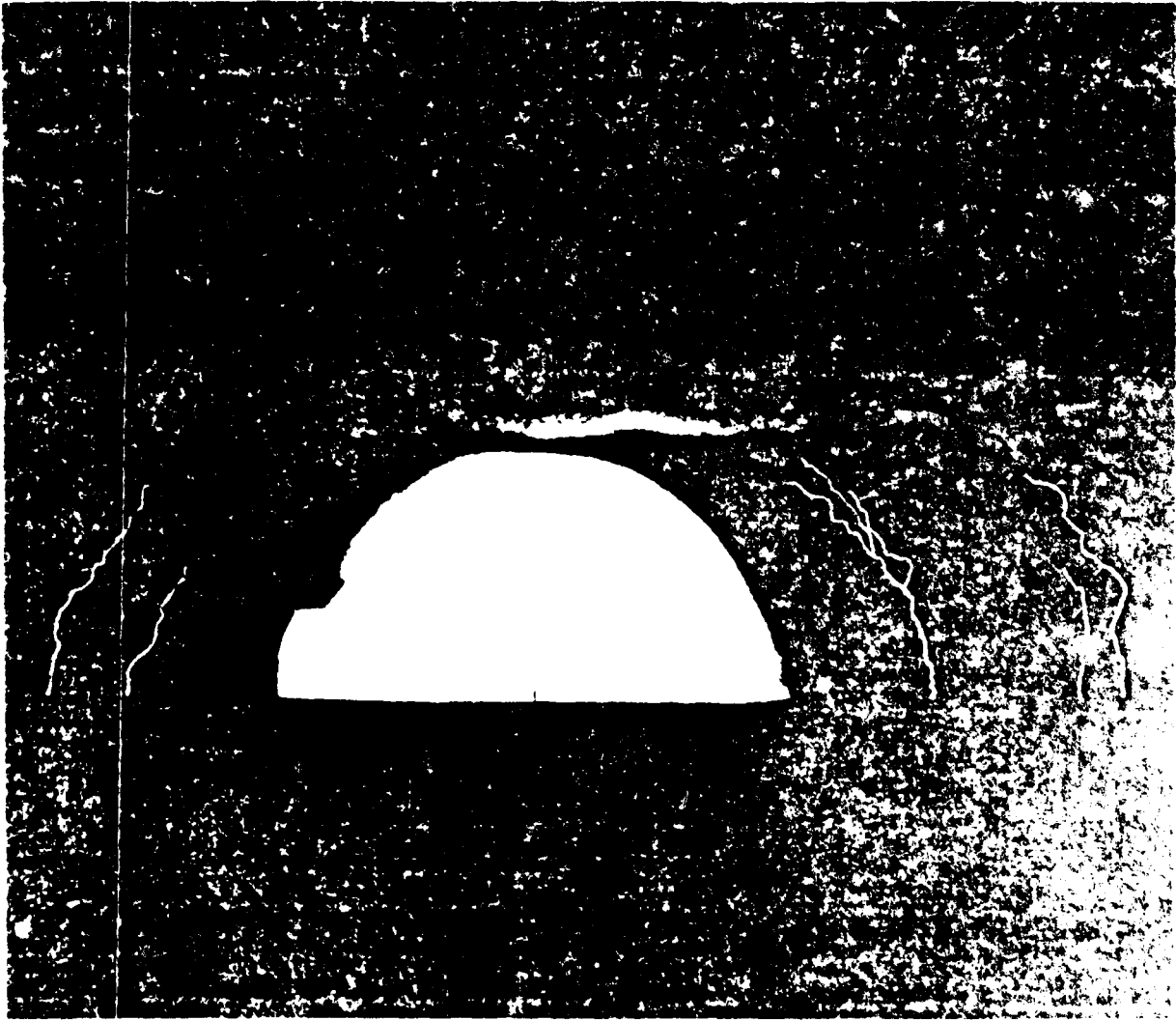


Figure 1. Lightning induced by a surface thermonuclear explosion in the Pacific. The five lightning channels have been inked for better reproduction.

For this reaction to compete with reaction 4 requires a concentration of HNO_3 of at least $2 \times 10^{15} \text{ cm}^{-3}$. As we shall see later, the amount of HNO_3 production is about 0.25 of Q , the total number of ion-pairs formed by the energy deposition ($Q = \int q dt$), when Q is less than or equal to 10^{16} cm^{-3} . Thus, if we have a Q equal to or greater than $8 \times 10^{15} \text{ cm}^{-3}$, the HNO_3 could contribute significantly to the electron attachment.

The first calculation was done using a total ionization of $7 \times 10^{16} \text{ cm}^{-3}$. This was based on use of gamma source and transport formulae for normal bombs, scaled to the Mike neutron yield. At this high value, the production of HNO_3 was only about 0.1 of Q but this was enough so that HNO_3 strongly dominated the electron attachment and yielded an electron density much below the value calculated using the usual model.

It was pointed out to us by Dr. Forrest Gilmore, however, that this value of Q was much too high for the Mike burst. Measurements taken during that particular shot show an anomalously low dose rate at 2300 meters³. Scaling this data³ yields roughly a Q at 10^{-2} sec. and 500 meters from the burst of $2 \times 10^{16} \text{ cm}^{-3}$. At 1000 meters, which is more representative of the distances of the lightning strokes, the value of Q would be about 10^{15} cm^{-3} . Thus, at this time, the attachment to HNO_3 is at least an order of magnitude too small to explain the lightning strokes observed during the Mike shot³.

Other mechanisms exist which may explain the lightning strokes. One possibility is that leader growth is enhanced because of substantial background ionization and negative ion detachment mechanisms. Another possibility is introduced by the fact that, due to the electron fields, the electrons in the EMP source region can be much more energetic than the atoms or molecules. Endothermic attachment reactions which are insignificant at ambient temperatures may become important at the elevated electron temperatures.

Even though the HNO_3 production has not provided an explanation for the lightning strokes, it can impact the electron density, conductivity and electric field distribution in the EMP source region and therefore deserves some further study. In the next section, we describe the calculations already made and the chemistry involved in the HNO_3 production. The following section deals with the possibility of the enhancement of attachment by hot electrons. The last section deals with our conclusions.

THE PRODUCTION OF HNO₃ IN THE EMP SOURCE REGION

The formation of HNO₃ is accomplished mainly by the reaction



Although this is a three body reaction, at sea level density, the reaction has begun to saturate and behaves more as a two body process⁴. The rate coefficient used in these calculations for reaction 6 was

$$k_6 = 1.1 \times 10^{-11} \left(\frac{300}{T}\right)^{1/2} \text{ cm}^3/\text{sec} . \quad (7)$$

The NO₂ available to form HNO₃ is formed from the atomic nitrogen which is produced by the initial energy deposition. About 1.2 nitrogen atoms are formed per ion pair. Some of this is in the form of N⁺ but the bulk is in the form of neutral nitrogen in the ground state, N(¹S), and is the first excited state, N(²D). Figure 2 is a schematic of the chemistry scheme used for the "odd nitrogen." The N(¹S) and N(²D) are the starting points, and the heavy arrow indicates major reaction paths. The dotted arrows indicate reaction paths for which the reaction rates and products are uncertain or unknown and where strong assumptions were made. The species shown along the connecting arrows are the reactants involved in the various reaction paths.

We see that the atomic nitrogen can react to form NO, N₂O, or N₂. The reactions forming N₂ and N₂O involve the reaction of atomic nitrogen and NO, NO₂ or N₁. If the total ionization is small and/or spread out over an extended period of time, these species concentrations are never very large simultaneously and the reformation of N₂ is minimal. When the total ionization is large, N₂ reformation is significant and there is less NO and NO₂ available to form HNO₃ and HNO₂ (which competes with HNO₃ for the available odd nitrogen). This is why the efficiency of HNO₃ production is decreased when the total ionization in our calculations is large (>10¹⁶ cm⁻³).

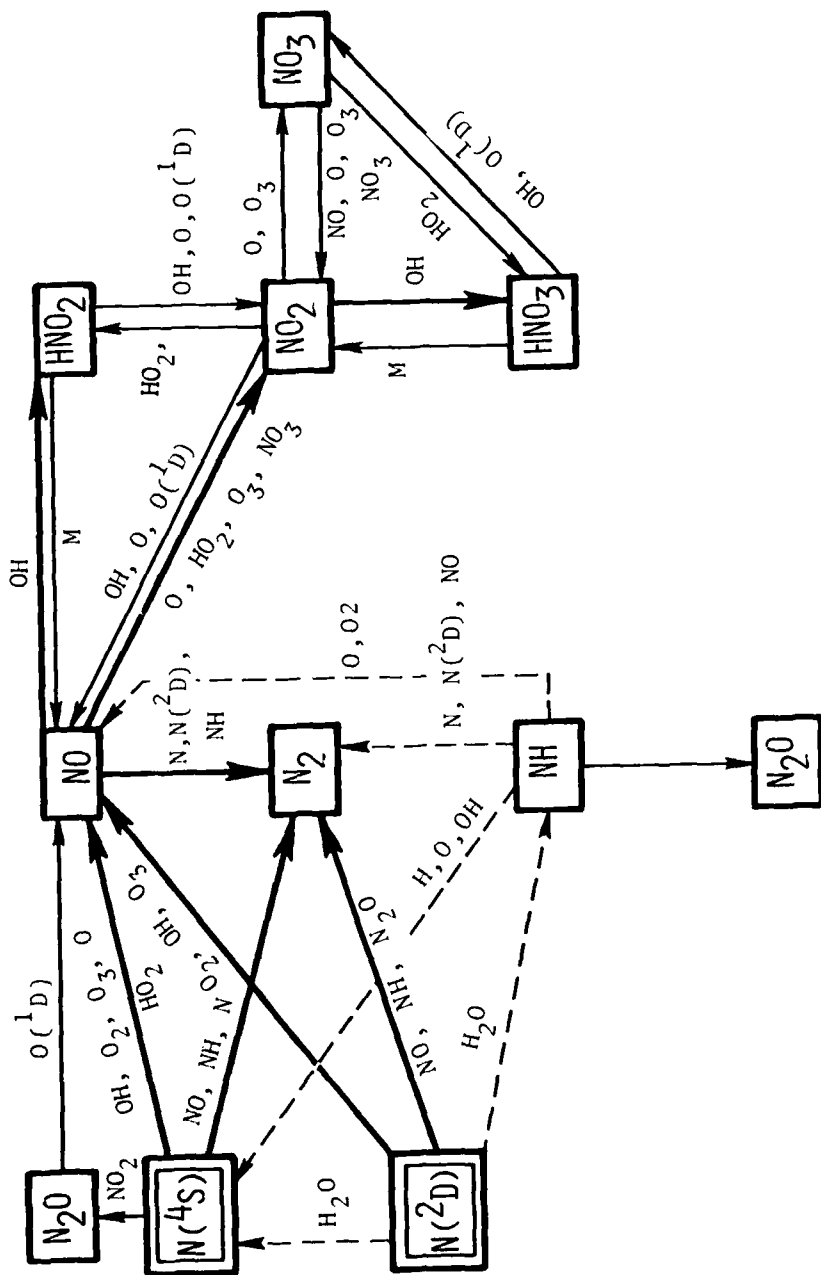


Figure 2. Odd nitrogen reaction scheme.

The critical reactions in this scheme are the formation of N_2 and NO from the atomic nitrogen, the oxidation of NO to NO_2 , in our case primarily by HO_2 , and the formation of HNO_2 and HNO_3 from NO and NO_2 by association with OH. The rate coefficients for these reactions are fairly well known. The role of NH, however, is uncertain. At sea level, virtually all the $N(^2D)$ formed is quenched by H_2O . The products have not been identified but probably are NH and OH. NH is known to react with NO with a rate constant of about $4 \times 10^{-11} \text{ cm}^3/\text{sec}$. but its reactions with N, O, H, OH and O_2 are unknown. With the exception of the reaction of NH with O_2 , we have assumed rate coefficients of the same order as the reaction with NO. The rate coefficient for the reaction with O_2 was assumed to be about a factor of 5000 smaller at 300K. These reactions and coefficients constitute the greatest uncertainty in the odd nitrogen reaction scheme and variations within the large area of uncertainty could significantly affect the eventual HNO_3 production.

Some of the H, OH, and HO_2 , or "odd hydrogen," is formed in the reactions of $N^2(D)$ and $O^1(D)$ (formed by the initial deposition of energy) with H_2O , and in the reactions of NH. The bulk, however, is formed in the process of positive ion hydration.

The ions formed initially are N^+ , O^+ , N_2^+ and O_2^+ . Prior to recombination, however, almost all of these ions are transformed into a series of more complex ions terminating with the hydronium ion H_3O^+ \cdot $(H_2O)_n$, where n can be very large. Figure 3 shows one of the schemes by which this occurs. Much of the N^+ , O^+ and N_2^+ reacts with various neutral species to form O_2^+ . The O_2^+ either directly or indirectly clusters to form $O_2^+ \cdot H_2O$, which then reacts with H_2O to form the hydronium cluster. There are other schemes, particularly one involving NO^+ , which lead to the hydronium ion, but the one shown is the most important under strongly disturbed condition.

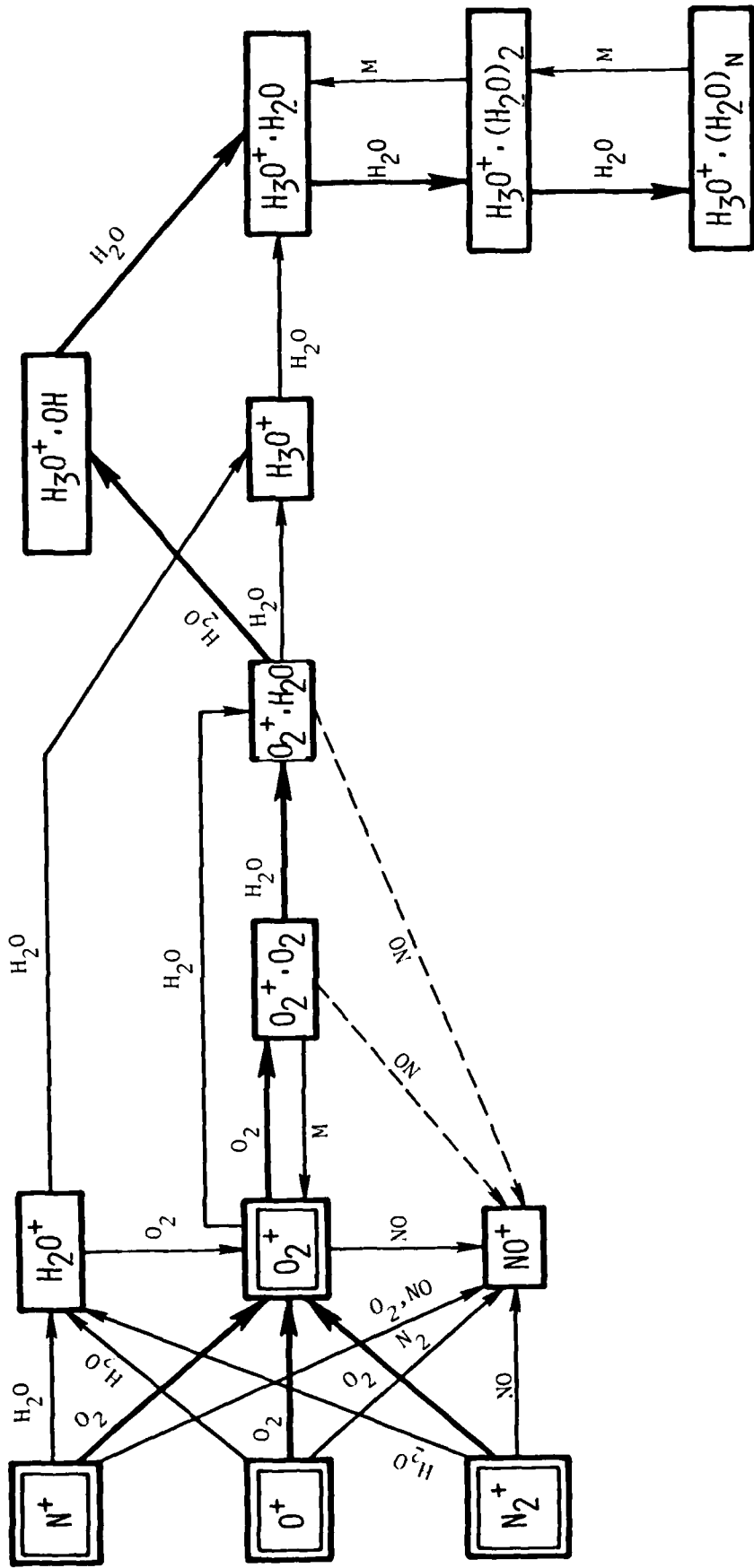


Figure 3. Formation of hydronium ions via O_2^+ .

It is obvious that, in the transformation of any of the initial ions to a cluster of H_3O^+ , an OH molecule is released. When the H_3O^+ cluster recombines, either with an electron or a negative ion, another odd hydrogen species is released. This is the major source of odd hydrogen in our problem. In the recombination of $\text{H}_3\text{O}^+ \cdot (\text{H}_2\text{O})_n$ we have assumed that a free hydrogen atom is released, the fate of which, almost always, is to associate with an O_2 molecule to form HO_2 . When recombining with negative ions, this may not be true. Species such as OH, HO_2 , HNO_2 and HNO_3 may be formed, depending on the negative ion, as a direct result of the charge neutralization process. The significance of this upon our problem has not yet been investigated.

Figure 4 is a schematic of the odd hydrogen chemistry scheme. The most critical reaction in this scheme is the reaction between OH and HO_2 to form H_2O and O_2 . This reaction is the main process by which the total odd hydrogen is depleted and H_2O reconstituted. The rate coefficient used in the calculations for this reaction was $2 \times 10^{-11} \text{ cm}^3/\text{sec}$. A larger rate coefficient is now being recommended⁴ ($4 \times 10^{-11} \text{ cm}^3/\text{sec}$). Increasing this rate coefficient will decrease the OH that is available to associate with NO_2 and thus could decrease the total HNO_3 production. Another area of uncertainty has already been mentioned in the last paragraph and concerns the fate of the hydrogen atom made available by the neutralization of the H_3O^+ cluster with various negative ions.

Figures 5 and 6 show the species concentrations as a function of time for a total ionization, Q , of 10^{16} ion pairs/ cm^3 . The specific ionization function used was

$$q = 10^{20} e^{-10^4 t} \text{ ion pairs/cm}^3 . \quad (8)$$

This function essentially "turns off" by 10^{-3} second. The time is measured from the arrival of the radiation at the point in question.

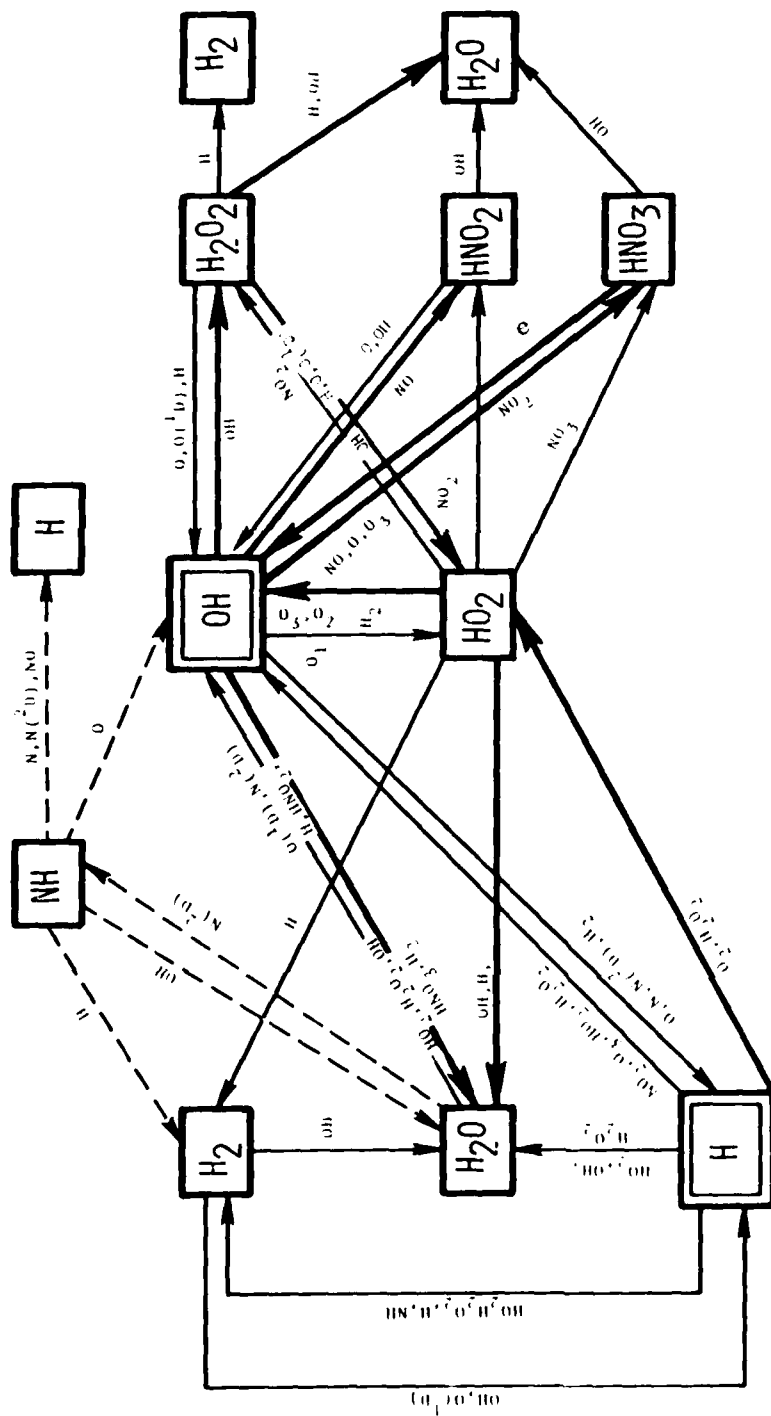


Figure 4. Odd hydrogen reaction scheme.

Figure 5 shows the odd hydrogen species plus H_2 and O_3 . Figure 6 shows the odd nitrogen species plus N_2O . We see that the important species OH and HO_2 rise rapidly to a maximum of about 10^{15} cm^{-3} as the ion hydration and recombination produces H and OH and the H associates with O_2 to form HO_2 . After a time of about 5×10^{-5} seconds, the ionization rate decreases significantly, and the reaction between OH and HO_2 to form H_2O and O_2 has an appreciable effect, causing the OH and HO_2 to decrease. Though these are the main determinants of the OH and HO_2 behavior, other reactions are appreciable, in particular, the reactions of OH or HO_2 with $N(^4S)$, O, NO and NO_2 . The first rise of the atomic hydrogen is due to its production by clustered hydronium ion recombination. The second rise is due to reactions of $N(^4S)$ and O with OH which adds to the production of H. The decrease of H after 5×10^{-5} seconds is predominantly due to the decrease of the ionization rate and the association of H with O_2 to form HO_2 . Hydrogen peroxide, H_2O_2 , is formed primarily by the association of two OH molecules. It reaches a value of about $2 \times 10^{15} \text{ cm}^{-3}$ at 2×10^{-4} seconds and remains approximately constant beyond that because of the decay of the OH. The ozone O_3 is shown because it is a significant oxidizer of NO and may play a role in electron attachment at high electron temperatures. It is formed primarily by association of O_2 with atomic oxygen. The slight decay after 10^{-3} seconds is due to its breakup by $O_2(^1\Delta)$, a long lived metastable state of oxygen produced by the energy deposition. Also shown in Figure 5 is H_2 which is formed by the reactions of H with HO_2 , NH and H_2O_2 .

The NO in Figure 6 is formed mainly by the reactions of $N(^2D)$ and NH with O_2 and the reactions of $N(^4S)$ with OH, O_2 and HO_2 . The decline after 10^{-4} seconds is due to those reactions which oxidize NO to NO_2 , or which form HNO_2 . The NO_2 rises rapidly after 10^{-6} seconds and levels off at a value of about $3 \times 10^{15} \text{ cm}^{-3}$ when the production of odd nitrogen ceases and the NO concentration drops. The behavior of the

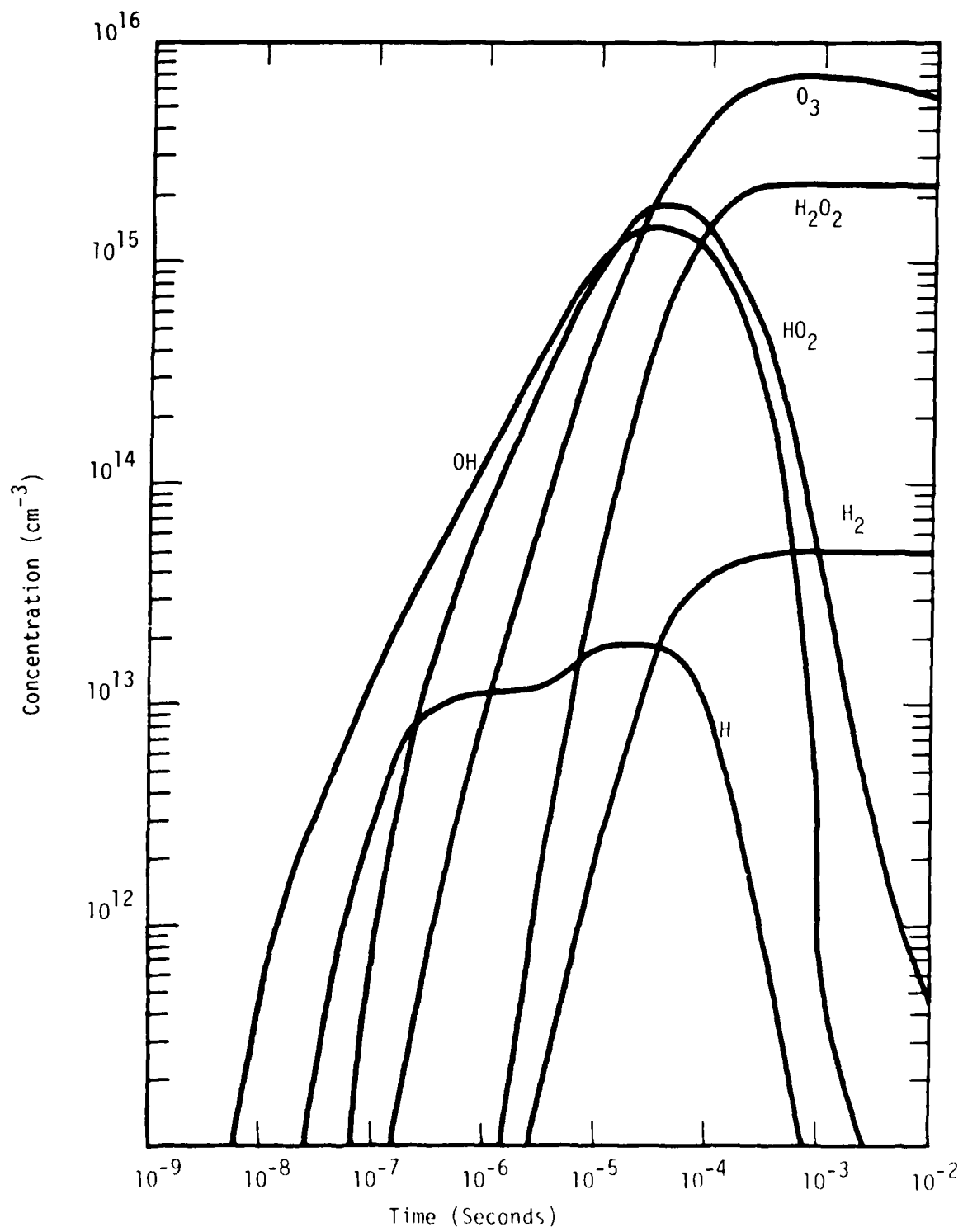


Figure 5. Odd hydrogen, H_2 and O_3 species concentrations.

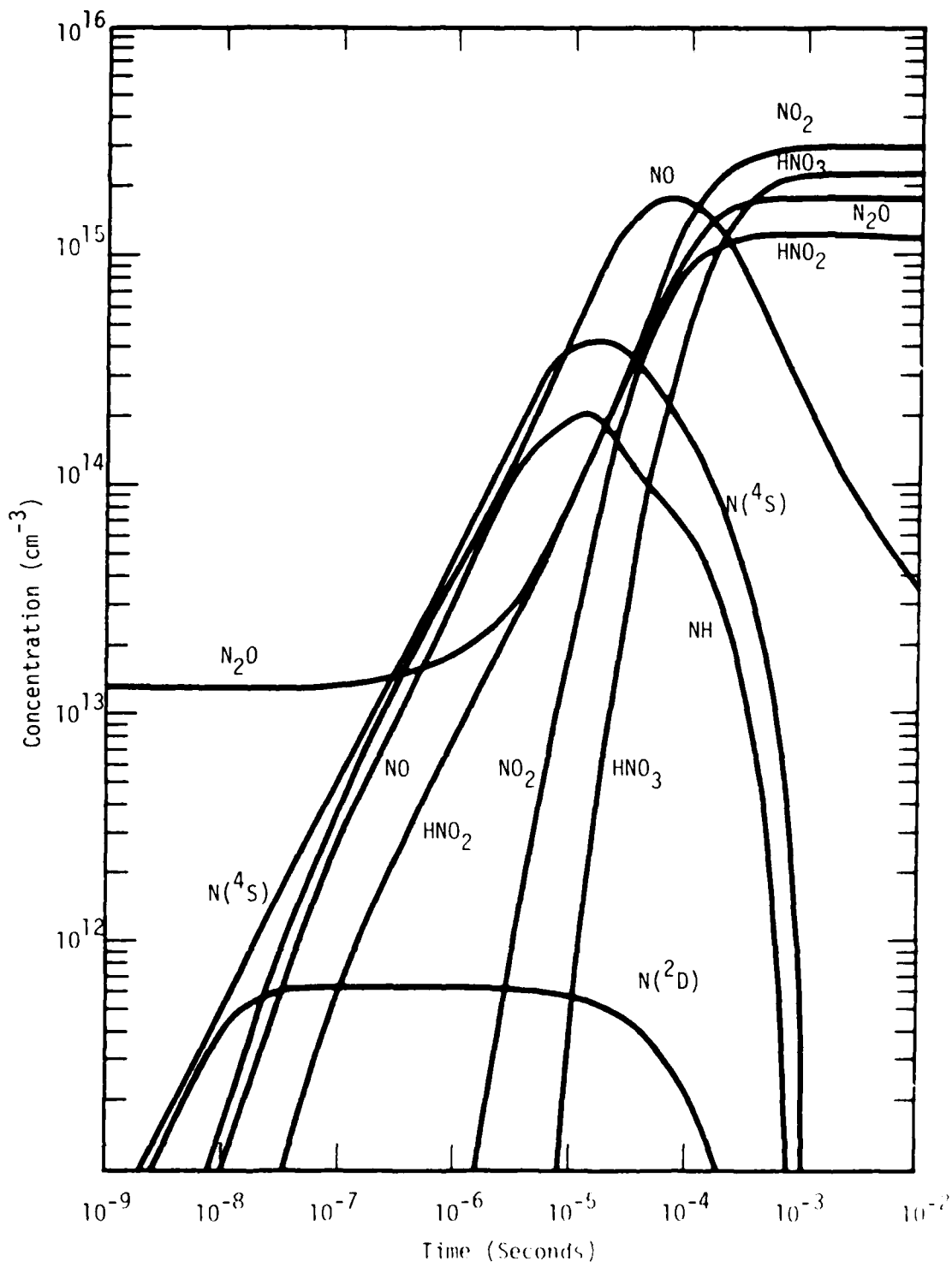


Figure 6. Odd nitrogen and N₂O species concentrations.

HNO_3 is similar to that of the NO_2 , from which it is formed. The leveling off at about $2.4 \times 10^{15} \text{ cm}^{-3}$ slightly before 10^{-5} seconds is due to the disappearance of the OH which is necessary for HNO_3 formation. The behavior of HNO_2 is very similar to that of HNO_3 except that significant quantities are formed earlier because of the presence of NO at these times. Figure 6 also shows the N_2O concentration which increases from an ambient value of $1.3 \times 10^{13} \text{ cm}^{-3}$ to a value of almost 2×10^{15} after 3×10^{-5} seconds. The N_2O is almost all produced by the reaction of $\text{N}(^4\text{S})$ with NO_2 and therefore ceases when the $\text{N}(^4\text{S})$ concentration becomes small.

This calculation was made using a water vapor concentration of 1 percent. Other calculations were made with this same water vapor concentration for different values of the total ionization from 10^{15} cm^{-3} to $7 \times 10^{16} \text{ cm}^{-3}$. As indicated in the introduction, below a value of about $2 \times 10^{16} \text{ cm}^{-3}$, the HNO_3 production is about 0.25 per ion pair. Above $2 \times 10^{16} \text{ cm}^{-3}$, the reactions reconstituting N_2 from the odd nitrogen species become important and the efficiency of HNO_3 production drops. At $7 \times 10^{16} \text{ cm}^{-3}$ total ionization, it is about 0.1 per ion pair.

A set of calculations were also made with a water vapor concentration of 1 percent. These showed very little difference in the HNO_3 concentrations with the 1 percent calculations. The basic reason for this is that at both water vapor concentrations virtually all of the ions formed transform to the hyronium clusters before recombination and virtually all of the $\text{N}(^2\text{D})$ reacts with H_2O rather than with O_2 . The water vapor concentration would have to be decreased to below 0.1 percent before any significant differences occur. At the lower water vapor concentrations, however, the attachment due to reaction 4 (attachment to O_2) when H_2O is the third body is decreased. Thus, since the HNO_3 concentrations are the same, the relative contribution of HNO_3 to the electron attachment is greater when the water vapor concentration is small.

At an integrated ionization value of 10^{16} cm^{-3} , we had a value for the HNO_3 concentration of $2.4 \times 10^{15} \text{ cm}^{-3}$ at 10^{-3} seconds. This yields a contribution to the attachment of $1.2 \times 10^8 \text{ sec}^{-1}$. The contribution from O_2 attachment when the H_2O relative concentration is 2 percent and the temperature is 350K (the energy deposited raises the temperature in this case about 55K) is $1.1 \times 10^8 \text{ sec}^{-1}$. Thus, the HNO_3 doubles the attachment and halves the electron density at this time. This is not enough to explain the lightning strokes in the Mike shot but is enough to cause significant effects in the EMP phenomena. At 500 km distance from the Mike burst, we had a Q of $2 \times 10^{16} \text{ cm}^{-3}$ at 10^{-2} seconds. This would give us an attachment rate a factor of three larger than is currently predicted.

The uncertainties involved in the NH reaction scheme and the ion-ion recombination have already been mentioned. Another possibly important uncertainty involves the role of photodissociation by bomblight. This not only applies to the photodissociation of HNO_3 but also to species such as NO_2 , HO_2 and O_3 . The photodestruction of NO_2 and HO_2 would interrupt the chain of reactions leading to the formation of HNO_3 . The photodissociation of O_3 would lead to a large atomic oxygen population at the times of interest. This atomic oxygen would react with HO_2 and NO_2 and further tend to deplete these species. Rough calculations indicate that at a kilometer distance photodissociation probably does not play a significant role. At 500 meters, however, it may have a significant effect. This and the other uncertainties should be investigated.

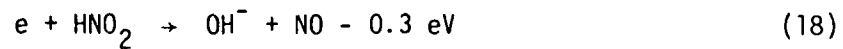
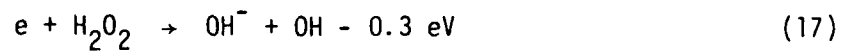
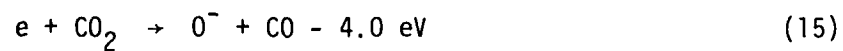
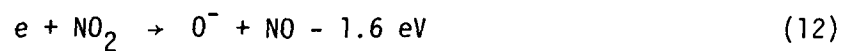
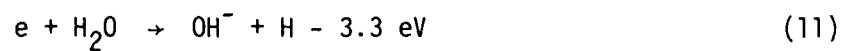
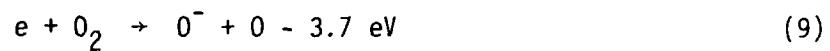
INCREASED ATTACHMENT DUE TO HOT ELECTRONS

Another possible source of increased attachment stems from the fact that in the EMP source region the electric fields which are generated are capable of heating the electrons to temperatures considerably above the ambient heavy particle temperature. Electron temperatures (the velocity distribution is not, strictly speaking, Maxwellian, but, except for the high energy tail, this is a fairly good assumption) of up to 1 eV are attainable and this opens up the possibility that a number of endothermic dissociative attachment reactions which are not significant at ambient temperatures may become so. A list of a number of these possibilities is shown in Table 1. Shown also are the energy changes involved in the reactions.

The reactions in Table 1 were chosen because the neutral reactants are either present in the ambient atmosphere in large amounts (O_2 , H_2O , and CO_2) or are produced copiously by the energy deposition and do not decay quickly after the ionization source is turned off, at least not in the time scale of less than a second. The rate coefficients of the reverse of reactions 9 to 15 have been measured, at least at room temperature, and this enables us to obtain rate coefficients for the forward reactions by detailed balancing. This, however, is done assuming that the reactants and products have Maxwellian velocity distributions and Boltzmann distributions in internal energy states. If the neutral species formed by the reverse of the reactions in Table 1 are preferentially produced in highly excited states, detailed balance will overestimate the rate coefficients of the forward reactions. What information that exists on the forward reactions indicates that this is the case, at least for some of the reactions.

The reactions 9 to 15 all have rate coefficients for the associative detachment reverse reactions between $1.5 \times 10^{-10} \text{ cm}^3/\text{sec}$ and $1.4 \times 10^{-9} \text{ cm}^3/\text{sec}$ at 300K^5 . Little is known about the temperature

Table 1. Endothermic dissociative attachment reactions



dependence of these rate coefficients. The rate coefficients of the forward dissociative attachment reactions, k_a , can be obtained from the reverse detachment rate coefficients, k_d , by the relation

$$k_a = k_d K_{eq} \left(\frac{T}{T_e} \right)^{2.5} \quad (19)$$

where T_e and T are the electron and molecular temperatures, K_{eq} is the equilibrium constant assuming all temperatures are equal, and the term in parentheses takes into account that T_e and T may be considerably different.

Of the reactions in Table 1, more experimental data is available for reaction 9 than any of the others. Use of equation 19 yields

$$k_9 = 3.4 \times 10^{-5} \left(\frac{300}{T} \right) \left(\frac{T}{T_e} \right)^{2.5} e^{-42400/T_e} \quad (20)$$

Taking $T = 300\text{K}$ and $T_e = 6000\text{K}$ and 12000K , we obtain values of k_9 of 2×10^{-11} and $10^{-10} \text{cm}^3/\text{sec}$, respectively. This yields attachment rates of 10^8 and $5 \times 10^8 \text{sec}^{-1}$, respectively, at sea level. The fact that the electron densities in the high energy tail of the velocity distribution are probably significantly larger than Maxwellian densities would further increase the attachment rates. The experimental data, however, does not support these values. The cross section data for reaction 9, for different O_2 temperatures and as a function of electron energies, are shown in Figure 7⁶. Using the curve for $T = 300\text{K}$, we obtain a value of k_9 of roughly $4 \times 10^{-14} \text{cm}^3/\text{sec}$ for $T_e = 6000\text{K}$ and 4×10^{-14} for $T_e = 12000\text{K}$. This is considerably less than obtained by detailed balance and almost certainly indicates that in the dissociative attachment of O^- by O (the reverse of reaction 9) the O_2 is produced in vibrationally excited states. This would explain the significantly increased cross sections in

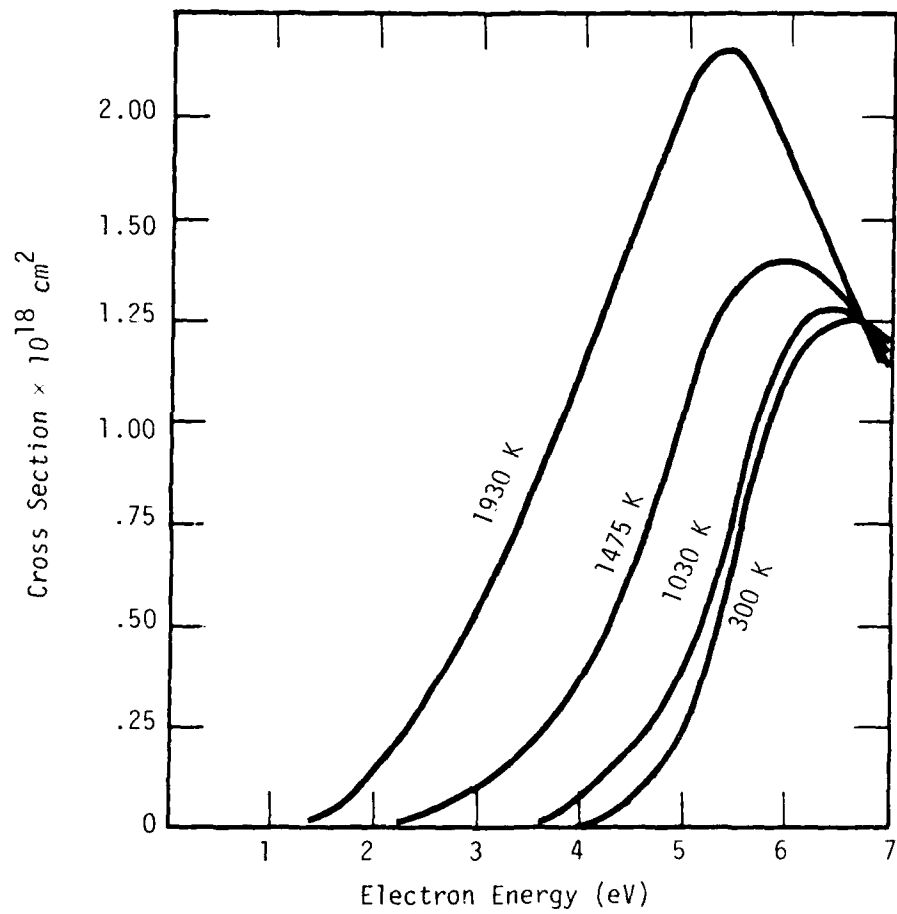


Figure 7. Cross sections for associative detachment to O₂.⁶

Figure 7 when the O_2 temperature is increased. When the O_2 temperature is 1930K, we obtain values of k_9 of $4 \times 10^{-12} \text{cm}^3/\text{sec}$ for $T_e = 6000\text{K}$ and $3 \times 10^{-11} \text{cm}^3/\text{sec}$ for $T_e = 12000\text{K}$. We see that we are getting into the O_2 temperature region in which dissociative attachment to O_2 may contribute significantly to the overall attachment.

The potential contribution of reaction 9 to the attachment depends, therefore, on whether a significant amount of vibrational excitation can be maintained over a period of time of up to one or more milliseconds. The rapid deactivation of vibration excited O_2 by H_2O ($1.7 \times 10^{-11} \text{cm}^3/\text{sec}$)⁶ makes this highly unlikely. Mechanisms such as vibration transfer from excited N_2 , or chemical reactions such as $O + O_3 \rightarrow O_2(^1\Delta) + O_2^\ddagger$, or excitation by electrons and ions accelerated by the electric field are not rapid enough to maintain the necessary amount of O_2 vibrational excitation against this large a deactivation rate.

The situation is similar for other reactions for which there are cross section data. The cross section data for dissociative attachment to CO_2 at 300K⁷ also yield a rate coefficient much less than that predicted by detailed balance. For N_2O , however, the cross section data⁷ yield values of k_{16} which, though small, are not greatly different than those one would expect from detailed balancing. One can hypothesize that this is due to the fact that the energy needed to make this reaction go is only 0.2 eV rather than the 3.7 and 4.0 eV needed for the reactions with O_2 and CO_2 (see Table 1). In a dissociative detachment reaction which is resonant using ground state energies, excited products will not likely be produced and one would then expect detailed balance to yield the correct rate coefficient for the attachment reaction. One could assume, therefore, that the closer the reaction is to resonance the more reliability one can place on detailed balance. This reasoning would seem to indicate that the last three reactions in Table 1 and reaction 14 would be the most promising. With only a little vibrational excitation and a moderate

electron temperature of a few tenths of an electron volt, these reactions might contribute significantly to the attachment rate.

There is no information concerning reactions 17 and 18, but the rate coefficient of the reverse of reaction 14 has been measured to be $1.5 \times 10^{-10} \text{ cm}^3/\text{sec}$ at 300K. By detailed balance, we obtain

$$k_{14} = 1.6 \times 10^{-4} \left(\frac{300}{T} \right) \left(\frac{T}{T_e} \right)^{5/2} \quad (21)$$

For $T = 300\text{K}$ and $T_e = 3000\text{K}$ we have $k_{14} = 5 \times 10^{-8}$. If we assume a value of one ozone molecule formed per ion pair produced (a reasonable value for Q between 10^{15} and 10^{16} cm^{-3}), we would have the attachment to O_3 equal to 10^8 sec^{-1} for $Q = 2 \times 10^{15} \text{ cm}^{-3}$. This is the Q we would expect about 900 meters from the Mike burst.

Again we must know whether vibrational excitation is involved and, if so, whether sufficient vibrational excitation can be maintained under our conditions. No information is available on whether O_3 is produced in a vibrationally excited state in the associative detachment of O_2^- by atomic oxygen, but it would be reasonable to assume that it is. Because the endothermicity is only 0.6 eV, however, we would not expect that vibrational excitation will be as important as in reaction 9. In addition, there is a possibility that an O_3 vibrational state distribution with a temperature higher than ambient can be maintained over much of the time of interest. The quenching rate coefficient of O_3^+ by N_2 and O_2 is about $2 \times 10^{-14} \text{ cm}^3/\text{sec}$ ⁸. The process which forms ozone, the three body association of atomic oxygen with O_2 , has a rate coefficient of about $7 \times 10^{-34} \text{ cm}^6/\text{sec}$ and also forms it with about five quanta of vibrational energy⁸. Once a steady state is attained, the amount of O_3^+ will be roughly equal to the atomic oxygen concentration. Thus, as long as the atomic concentration is a significant fraction of the O_3 concentration, the O_3 will be significantly excited.

The measurements made during the Mike shot can be interpreted as indicating that the prompt pulse of ionizing radiation lasts more like 10^{-2} second rather than the 10^{-3} second we have assumed in our calculations. This would extend in time the production of atomic oxygen and result possibly in a significant ozone excitation out to times of the order of milliseconds.

The attachment to H_2O_2 and HNO_2 involves about half the amount of energy difference than the attachment to O_3 and therefore should be even less sensitive to the need for vibrational excitation. Attachment cross section information is needed for these species and O_3 , preferably as a function of both electron energy and molecular temperature.

CONCLUSIONS

Though the attachment to HNO_3 cannot, at this point, explain the lightning strokes observed during the Mike shot, it nevertheless may play a role in determining the electron density and conductivity in the EMP source region. From the calculations made to date, the efficiency of HNO_3 production is about 0.25 per ion pair for total ionization levels below about $2 \times 10^{16} \text{ cm}^{-3}$. The contribution to the effective attachment coefficient is given by

$$\Lambda_{\text{HNO}_2} \approx 10^{-8} Q \text{ sec}^{-1} \quad (22)$$

A more careful study of the uncertainties involved may change this number. In particular, the effect of photodissociation by bomblight may decrease this number appreciably at distances close to the burst point.

The possibility exists that the total electron attachment may also be augmented significantly by dissociative attachment reactions which are endothermic. This is brought about by the fact that the electric field generated within the EMP source region heats the free electrons to temperatures appreciably higher than ambient temperature. The data which exist indicate, however, that the attachment rate coefficient is highly sensitive to the degree of vibration excitation in the molecule, particularly if the energy difference is large. This would seem to rule out species such as O_2 , H_2O and CO_2 as good attachers in our case. The strong possibility exists that when the energy difference is small, such as with O_3 , H_2O_2 and HNO_2 , the rate coefficient is not critically dependent on the vibrational excitation of the molecule. This is particularly true of H_2O_2 and HNO_2 , but nothing is known about these attachment rates.

Some further investigation is needed regarding HNO_3 production in the EMP source region. The effect of the uncertainties associated with the NH reactions and ion-ion recombination products should be studied as well as the effect of photodissociation by bomb light.

In the area of associative attachment, a study should be made to determine the specific electron velocity distributions in air brought about by different electric field strengths. The effect of collisions with the species produced by the radiation should be included. Particular attention should be placed on the high energy tail of the distribution. With this information available, a quantitative evaluation is possible to determine what cross sections are needed for various species to make them important in the attachment process. If these cross sections are reasonable, recommendations for experimental studies can be made.

REFERENCES

1. Uman, M. A., et al., JGR, 77, p. 1591, 1972.
2. Fehsenfeld, F. C., et al., JCP, 63, p. 2835, 1975.
3. Scheibe, M. and C. Longmire, The Effect of Ionization-Induced SMOG on EMP Environments, MRC-N-362, Mission Research Corporation, Santa Barbara, California, February 1979.
4. DeMore, W. B., et al., Chemical Kinetic and Photochemical Data for Use in Stratospheric Modelling, JPL Publication 79-27, Jet Propulsion Laboratory, Pasadena, California, April, 1979.
5. DNA Reaction Rate Handbook, DNA 1948H, March 1972 (plus revisions).
6. Henderson, W. R., et al., Phys. Rev., 183, p. 157, 1969.
7. Rapp, D. and D. D. Briglia, JCP, 43, p. 1480, 1965.
8. von Rosenberg Jr., C. W. and D. W. Trainer, JCP, 61, p. 2442, 1974.

DISTRIBUTION LIST

DEPARTMENT OF DEFENSE

Assistant to the Secretary of Defense
Atomic Energy
ATTN: Executive Assistant

Defense Advanced Rsch. Proj. Agency
ATTN: TIO

Defense Nuclear Agency
2 cy ATTN: RAAE
4 cy ATTN: TITL

Defense Technical Information Center
12 cy ATTN: DD

Field Command
Defense Nuclear Agency
ATTN: FCPR

Field Command
Defense Nuclear Agency
Livermore Division
ATTN: FCPRL

Interservice Nuclear Weapons School
ATTN: TTV

Undersecretary of Def. for Rsch. & Engrg.
ATTN: Strategic & Space Systems (OS)

DEPARTMENT OF THE ARMY

Atmospheric Sciences Laboratory
U.S. Army Electronics R&D Command
ATTN: DELAS-EO-ME, K. Ballard
ATTN: DELAS-EO, F. Niles
ATTN: DELAS-EO-MO, M. Heaps

BMD Advanced Technology Center
Department of the Army
ATTN: ATC-T, M. Capps
ATTN: ATC-O, W. Davies

Harry Diamond Laboratories
Department of the Army
ATTN: DELHD-N-P
ATTN: DELHD-I-TL
ATTN: DELHD-I-TL, M. Weiner

U.S. Army Ballistic Research Labs.
ATTN: DRDAR-BLB, M. Kregel
ATTN: DRDAR-BLP, J. Heimerl
ATTN: DRDAR-BLT, J. Vanderhoff
ATTN: DRDAR-TSB-S

U.S. Army Foreign Science & Tech. Ctr.
ATTN: DRXST-SD-3

U.S. Army Missile Command
ATTN: Redstone Scientific Info. Ctr.

U.S. Army Nuclear & Chemical Agency
ATTN: Library

U.S. Army Research Office
ATTN: R. Mace

DEPARTMENT OF THE ARMY (Continued)

U.S. Army TRADOC Systems Analysis Activity
ATTN: ATAA-PL

White Sands Missile Range
Department of the Army
ATTN: STEWS-TE-AN, M. Squires

DEPARTMENT OF THE NAVY

Naval Electronic Systems Command
ATTN: PME 117-20
ATTN: Code 501A
ATTN: ELEX 03

Naval Intelligence Support Ctr.
ATTN: Document Control

Naval Ocean Systems Center
ATTN: Code 5322, H. Hughes
ATTN: Code 5321, I. Rothmuller
ATTN: Code 532, R. Pappert
ATTN: Code 532, J. Richter
ATTN: Code 5324, W. Moler
ATTN: Code 4471

Naval Postgraduate School
ATTN: Code 0142, Library

Naval Research Laboratory
ATTN: Code 7550, J. Davis
ATTN: Code 6750, D. Strobel
ATTN: Code 2627
ATTN: Code 7101, P. Mange
ATTN: Code 7122, D. McNutt
ATTN: Code 6780, J. Fedder
ATTN: Code 4700, T. Coffey
ATTN: Code 6750, K. Hain
ATTN: Code 7175, J. Johnson
ATTN: Code 7175H, D. Horan
ATTN: Code 4780, S. Ossakow
ATTN: Code 1434, E. Brancato
ATTN: Code 4709, W. Ali
ATTN: Code 7120, R. Kinzer
ATTN: Code 4701, J. Brown

Naval Surface Weapons Center
ATTN: L. Rudlin
ATTN: Code F31
ATTN: Code R41, D. Land
ATTN: Code F46, D. Hudson

Nuclear Weapons Tng. Group, Pacific
ATTN: Nuclear Warfare Department

Office of Naval Research
ATTN: Code 465, G. Joiner
ATTN: Code 421, B. Junker

DEPARTMENT OF THE AIR FORCE

Air Force Technical Applications Center
ATTN: TD
ATTN: TF, L. Seiler
ATTN: STINFO Office/TF

DEPARTMENT OF THE AIR FORCE (Continued)

Air Force Geophysics Laboratory
ATTN: LKB, W. Swider, Jr.
ATTN: OPR-1, J. Ulwick
ATTN: SULL
ATTN: LKB, T. Keneshea
ATTN: LKB, E. Murad
ATTN: LKB, J. Paulson
ATTN: LKB, K. Champion
ATTN: LKO, R. Van Tassel
ATTN: LKD, C. Philbrick
ATTN: LKD, R. Narcisi
ATTN: PHG, F. Innes
ATTN: OPR, F. Delgreco
ATTN: LKO, R. Huffman
ATTN: OP, J. Garing
ATTN: OPR, A. Stair
ATTN: OPR, T. Connolly
ATTN: OPR, H. Gardiner
ATTN: OPR, J. Kennealy
ATTN: OPR, R. Oneill

Air Force Weapons Laboratory
Air Force Systems Command
ATTN: SUL
ATTN: DVV, E. Copus

Foreign Technology Division
Air Force Systems Command
ATTN: NIS Library
ATTN: WE

Rome Air Development Center
Air Force Systems Command
ATTN: OCS, V. Coyne
ATTN: OCSA, J. Simons

USAFETAC
ATTN: CBTL STOP 825

DEPARTMENT OF ENERGY CONTRACTORS

EG&G, Inc.
Los Alamos Division
ATTN: P. Lucero
ATTN: D. Wright
ATTN: J. Colvin

Lawrence Livermore National Laboratory
ATTN: L-71, J. Chang

Los Alamos National Scientific Laboratory
ATTN: MS 212, W. Barfield
ATTN: MS 668, H. Hoerlin
ATTN: MS 560, W. Hughes
ATTN: MS 668, J. Malik
ATTN: MS 664, J. Zinn

Sandia National Laboratories
ATTN: ORG 1250, W. Brown
ATTN: ORG 4241, T. Wright

OTHER GOVERNMENT AGENCIES

Research Director
Bureau of Mines
ATTN: J. Murphy

OTHER GOVERNMENT AGENCIES (Continued)

Department of Commerce
National Bureau of Standards
ATTN: W. Lineberger
ATTN: S. Leone
ATTN: A. Phelps

Department of Commerce
National Bureau of Standards
ATTN: J. Cooper
ATTN: L. Gevantman
ATTN: M. Krauss
ATTN: M. Scheer
ATTN: S. Abramowitz
ATTN: R. Hampson, Jr.
ATTN: J. Devoe
ATTN: D. Lide
ATTN: D. Garvin

Department of Commerce
National Oceanic & Atmospheric Admin.
ATTN: L. Machta
ATTN: J. Angell

Department of Commerce
National Oceanic & Atmospheric Admin.
ATTN: Assistant Administrator, RD

Department of Commerce
National Oceanic & Atmospheric Admin.
ATTN: E. Ferguson
ATTN: W. Spjeldvik
ATTN: F. Fehsenfeld
ATTN: D. Albritton

Department of Transportation
ATTN: F. Marmo

NASA
Goddard Space Flight Center
ATTN: S. Bauer
ATTN: Technical Library
ATTN: Code 625, J. Heppner
ATTN: Code 625, M. Sugiura
ATTN: J. Vette
ATTN: A. Aikin

NASA
George C. Marshall Space Flight Center
ATTN: W. Roberts

NASA
ATTN: R. Schiffer
ATTN: E. Schmerling
ATTN: D. Dement
ATTN: N. Roman

NASA
Johnson Space Center
ATTN: Code JM6, Technical Library

NASA
Ames Research Center
ATTN: G. Poppoff
ATTN: W. Starr
ATTN: N-245-3, R. Whitten

National Science Foundation
ATTN: R. Sinclair
ATTN: Div. of Atmos. Sci., R. McNeal

DEPARTMENT OF DEFENSE CONTRACTORS

Aero-Chem Research Labs., Inc.
ATTN: A. Fontijn

Aerodyne Research, Inc.
ATTN: F. Bien
ATTN: M. Faist
ATTN: M. Camac
ATTN: Librarian, B. Duston

Aeronautical Rsch. Assoc. of Princeton, Inc.
ATTN: H. Pergament

Aerospace Corp.
ATTN: L. Brary
ATTN: I. Taylor
ATTN: H. Mayer
ATTN: Library
ATTN: R. Cohen
ATTN: M. Whitson

University of Alaska
ATTN: N. Brown
ATTN: R. Parthasarathy
ATTN: Technical Library

AVCO Everett Research Lab., Inc.
ATTN: C. Von Rosenberg, Jr.

Berkeley Research Associates, Inc.
ATTN: J. Workman

Boston College
ATTN: Chairman, Dept. of Physics
ATTN: Science Library, F. McElroy
ATTN: Dept. of Chemistry, D. McFadden

University of California at San Diego
ATTN: D. Miller

University of California at Santa Barbara
ATTN: M. Steinberg

California Institute of Technology
ATTN: V. Anicich
ATTN: S. Trajmar

University of California
ATTN: H. Johnston

Calspan Corp.
ATTN: W. Wurster
ATTN: Library
ATTN: C. Treanor

Chem Data Research
ATTN: K. Schofield

University of Colorado
ATTN: Dept. of Chemistry, V. Bierbaum

Columbia University
ATTN: Security Officer for H. Foley

University of Denver
ATTN: Security Officer for D. Murcay
ATTN: Security Officer for B. Van Zyl

Epsilon Labs., Inc.
ATTN: C. Accardo

DEPARTMENT OF DEFENSE CONTRACTORS (Continued)

ESL, Inc.
ATTN: W. Bell

General Electric Co.
ATTN: M. Linevsky
ATTN: P. Zavitsanos
ATTN: Technical Information Center
ATTN: R. Edsall
ATTN: J. Peden
ATTN: J. Burns
5 cy ATTN: T. Bauer
6 cy ATTN: M. Bortner

General Electric Co.
ATTN: J. Schroeder

General Electric Company—TEMPO
ATTN: T. Stevens
ATTN: M. Stanton
ATTN: M. Dudash
ATTN: D. Chandler
ATTN: B. Gambill
ATTN: DANIA
ATTN: W. Knapp
ATTN: J. Thompson
ATTN: D. Reitz

General Research Corp.
ATTN: J. Iso, Jr.

General Research Corp.
ATTN: T. Zakrzewski

Howard University
ATTN: W. Jackson

HSS, Inc.
ATTN: M. Shuler
ATTN: D. Hansen

Information Science, Inc.
ATTN: W. Dudzial

Institute for Defense Analyses
ATTN: I. Bauer
ATTN: H. Wolthard

Ion Physics Corp.
ATTN: C. Bauer

IRT Corp.
ATTN: D. Vroom
ATTN: J. Rutherford
ATTN: R. Overmyer
ATTN: R. Neynaber

Johns Hopkins University
ATTN: J. Kaufman

Kaman Sciences Corp.
ATTN: D. Foxwell
ATTN: W. Rich

KMS Fusion, Inc.
ATTN: Library

DEPARTMENT OF DEFENSE CONTRACTORS (Continued)

Lockheed Missiles & Space Co., Inc.

ATTN: J. Reagan
ATTN: B. McCormac
ATTN: T. James
ATTN: J. Evans
ATTN: R. Sears
ATTN: R. Gunton
ATTN: J. Kumer
ATTN: M. Walt

Lockheed Missiles & Space Co., Inc.

ATTN: D. Divis

University of Lowell

ATTN: G. Best

M.I.T. Lincoln Lab.

ATTN: B. Watkins

University of Maryland

ATTN: Chemistry Dept., J. Vanderslice

University of Massachusetts

ATTN: H. Sakai

University of Minnesota

ATTN: J. Winkler

University of Minnesota

ATTN: M. Hirsch

Mission Research Corp.

ATTN: M. Messier
ATTN: D. Archer
ATTN: R. Kilb
ATTN: V. Van Lint
ATTN: M. Scheibe
ATTN: W. White
ATTN: D. Sappenfield
ATTN: R. Hendrick
5 cy ATTN: Document Control

National Academy of Sciences

ATTN: J. Sievers

State University of New York at Buffalo

ATTN: G. Brink

Nichols Research Corp., Inc.

ATTN: N. Byrn

Pacific-Sierra Research Corp.

ATTN: E. Field, Jr.

Panametrics, Inc.

ATTN: B. Sellers

Pennsylvania State University

ATTN: J. Nisbet
ATTN: L. Hale

PhotoMetrics, Inc.

ATTN: I. Kofsky

Physical Science Lab.

ATTN: W. Berning

Quantum Systems, Inc.

ATTN: S. Ormonde

DEPARTMENT OF DEFENSE CONTRACTORS (Continued)

Physical Sciences, Inc.

ATTN: K. Wray
ATTN: G. Caledonia
ATTN: R. Taylor

University of Pittsburgh

ATTN: F. Kaufman
ATTN: W. Fite
ATTN: M. Biondi

R & D Associates

ATTN: B. Gabbard
ATTN: H. Dry
ATTN: R. Lelevier
ATTN: R. Turco
ATTN: F. Gilmore
ATTN: C. MacDonald
ATTN: P. Haas

R & D Associates

ATTN: B. Yoon
ATTN: J. Rosengren
ATTN: H. Mitchell

Radiation Research Associates, Inc.

ATTN: N. Schaeffer

Rand Corp.

ATTN: C. Crain

Science Applications, Inc.

ATTN: D. Hamlin

Science Applications, Inc.

ATTN: N. Byrn

Science Applications, Inc.

ATTN: R. Johnston

Professor Chalmers F. Sechrist

University of Illinois

ATTN: S. Bowhill
ATTN: C. Sechrist

SRI International

ATTN: D. Hildenbrand
ATTN: E. Kindermann
ATTN: G. Black
ATTN: J. Moseley
ATTN: J. Peterson
ATTN: M. Baron
ATTN: R. Hake, Jr.
ATTN: R. Leadabrand
ATTN: T. Slanger
ATTN: V. Wickwar
ATTN: A. Whitson
ATTN: A. Peterson

SRI International

ATTN: C. Hulbert

Technology International Corp.

ATTN: W. Boquist

Teledyne Brown Engineering

ATTN: R. Deliberis

University of Texas System

ATTN: J. Browne

DEPARTMENT OF DEFENSE CONTRACTORS (Continued)

TRW Defense & Space Sys. Group
ATTN: J. Frichtenicht
ATTN: Technical Information Center

Utah State University
ATTN: K. Baker

University of Virginia
ATTN: H. Kelly
ATTN: R. McKnight
ATTN: R. Ritter

Visidyne, Inc.
ATTN: C. Humphrey
ATTN: H. Smith
ATTN: O. Manley
ATTN: T. Degges
ATTN: J. Carpenter

DEPARTMENT OF DEFENSE CONTRACTORS (Continued)

University of Washington
ATTN: Physics FM15, K. Clark

Wayne State University
ATTN: P. Ro1
ATTN: R. Kummler

Westinghouse Electric Corp.
ATTN: P. Chantry

William Marsh Rice University
ATTN: R. Stebbings

William Marsh Rice University
ATTN: J. Chamberlain

Johns Hopkins University
ATTN: Document Librarian